

Chapter 15

In-Silico Models of Trabecular Bone: A Sensitivity Analysis Perspective

Marlène Mengoni, Sebastien Sikora, Vinciane d'Otreppe,
Ruth Karen Wilcox and Alison Claire Jones

Abstract This chapter provides an overview from a sensitivity analysis perspective of computational mechanical modeling of trabecular bone, where models are generated from Computed Tomography images. Specifically, the effect of model development choices on the model results is systematically reviewed and analyzed for both micro-Finite Element and continuum-Finite Element models. Particular emphasis is placed on the image processing effects (thresholding, down-sampling, image to material properties relationships), the mesh-related aspects (mesh size, element type), and the computational representation of the boundary conditions. Typical issues are highlighted and recommendations are proposed with respect to various model applications, including global stiffness/strength and local failure stress/strain behavior.

Keywords Image-based FE models · Trabecular bone · Boundary conditions · Image processing · Numerical convergence

15.1 Introduction

Biological processes such as bone and soft tissue remodeling are triggered or influenced by the local mechanical environment through the cells' mechanotransduction [9, 57]. An accurate model of that environment is therefore important to capture the coupled mechano-biological response of biological tissues. In particular, this chapter will focus on the structural modelling of trabecular bone, which is a driver in applications such as bone adaptation and repair [8, 41]. There is wide-spread interest in replicating the behavior of trabecular bone within a computational environment.

M. Mengoni (✉) · S. Sikora · R.K. Wilcox · A.C. Jones
Institute of Medical and Biological Engineering, School of Mechanical Engineering,
University of Leeds, Leeds, UK
e-mail: m.mengoni@leeds.ac.uk

M. Mengoni · V. d'Otreppe
Department of Aerospace and Mechanical Engineering, Non-Linear
Computational Mechanics (LTAS-MN²L), University of Liege, Liège, Belgium

© Springer International Publishing Switzerland 2016
L. Geris and D. Gomez-Cabrero (eds.), *Uncertainty in Biology*,
Studies in Mechanobiology, Tissue Engineering and Biomaterials 17,
DOI 10.1007/978-3-319-21296-8_15

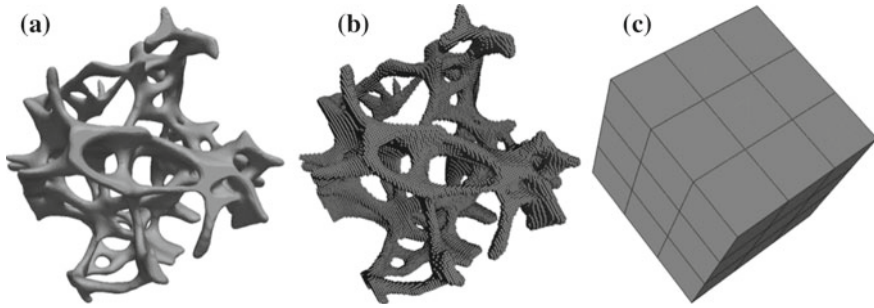


Fig. 15.1 Trabecular core of a deer antler (2.11 mm cubic specimen): **a** 3D visualization obtained from micro-CT images, **b** hexahedral micro-FE mesh (195,862 elements), and **c** hexahedral continuum-FE mesh (27 elements)

The improvement of bone strength estimation is a key clinical driver, which would enhance treatment of patients whose bones are weakened, such as those with osteoporosis. In parallel, researchers are developing detailed theoretical models of bone structure, material properties and macroscopic behavior in order to better understand its fracture mechanics and regeneration mechanisms.

The development of these patient-specific, highly detailed computer models of trabecular bone has been made possible by high-resolution, bench-top imaging systems such as micro-Computed Tomography (micro-CT) scanners. The three-dimensional images generated by a micro-CT scanner can be processed to extract geometric details at a macroscopic and microscopic level as well as maps of how the material properties vary throughout the bone.

This chapter reviews two of the dominant approaches to image-based modeling of trabecular bone. These are micro-Finite Element (micro-FE) models, which explicitly represent the micro-structure of the bone, and continuum-Finite Element models, which use a continuous, inhomogeneous material property field to implicitly represent that micro-structure (see Fig. 15.1).

Any theoretical representation of a physical system is built upon a series of assumptions about the behavior of that system. Finite element models of trabecular bone by necessity use boundary conditions and loading regimes which are either pure assumption or approximations of experimental conditions [42]. In addition the geometry, and in some cases the material properties, are derived from image data using theoretical relationships, calibrated conversion values, or user-controlled processes.

This chapter is specifically concerned with the sensitivity of key trabecular bone measures to the variation caused by modeling assumptions and decisions made during the derivation of geometries and material properties. Analysis of these sensitivities is a fundamental part of the model development process [18]. Data from the literature is reviewed and specific cases from the authors' work are used to provide more detailed examples.

15.1.1 Micro-Finite Element Models

Trabecular bone models which fall into the category of micro-FE explicitly include individual trabecular struts resolved as part of the three-dimensional model geometry. The element size within the mesh is small enough for several elements to span the thickness of a typical trabecular strut. The marrow and blood within the bone are generally excluded from the finite element mesh.

Due to the large number of elements and complex geometries, micro-FE models of trabecular bone typically require a large amount of computing resource and are often analyzed on high performance computers. With the advances in imaging techniques as well as computational power, micro-FE models have emerged since the 1990s. The high computational cost however generally restricts the size of samples which are processed, a typical area of bone represented is $(5\text{--}10\text{ mm})^3$ [50].

In some cases the trabecular bone within a micro-FE model may be assigned homogeneous material property constants across all elements [55]. In other cases the material properties are assigned on an element-by-element basis, using information from a micro-CT image [5, 25].

In order to construct a subject-specific micro-FE model of trabecular bone a three-dimensional image must be available with a resolution small enough to capture the trabecular geometry. Although bench-top micro-CT scanners can generate sufficiently high-resolution images, they are limited to relatively small in vitro specimens: a whole human vertebra can currently be scanned but generally not a complete human femur. In vivo imaging is possible through the use of high resolution peripheral Quantitative Computed Tomography (HR-pQCT) which makes it possible to capture trabecular level images of small peripheral human joints.

15.1.2 Continuum Finite Element Models

Continuum finite element models of trabecular bone use an element size which is too large for individual trabeculae to be resolved. A single element will typically cover an area which is large enough to contain several trabecular struts and the marrow space between them. Since fewer elements are needed, whole bone models can be analyzed at relatively low computational cost.

The trabecular structure within each element can be represented by a separate material property definition, creating a continuous but inhomogeneous map of properties throughout the bone. The sophistication and accuracy of the element-specific material models depends on both the source image and the modeling approach. In many cases the material properties are isotropic [22]. However, information on trabecular directionality has been used to derive orthotropic material properties for each element [37, 58].

15.1.3 Trabecular Bone Modeling Applications

Both the micro- and the continuum-FE modeling methods are capable of replicating apparent load-displacement behavior of trabecular bone, equivalent to the measurements obtained from a materials testing machine. In the case of continuum-FE, stiffness and strength of whole bones can be modeled [22, 27, 32, 44]. However, the use of a relatively low mesh density, which does not capture individual trabecular struts, limits the possible outputs to those at a macro level. Since micro-FE models are capable of capturing deformation of individual trabecular members, their outputs can include stress, strain and failure initiation within the microstructure.

The development of image-based computer modeling of bone has largely been driven by the need to assess the integrity of bone in patients with a suspected fracture risk. This may be to diagnose bone weakening conditions such as osteoporosis or metastatic involvement, or to measure the effectiveness of on-going treatment [3, 24, 48]. Models designed for this purpose generally use continuum material properties due to the low resolution of in vivo scanning. The apparent stiffness and strength measurements taken from these models have been compared to traditional DEXA scans in terms of reliability in predicting fracture [7].

The continuum-FE method has also been used in pre-clinical research setting to compare the effect of treatment across a set of specimens [54]. High resolution micro-CT source images may be available in the laboratory environment and can enhance the accuracy of continuum-FE models while the computational cost of the model solution remains low.

Where the high resolution imaging was available, micro-FE modeling has been developed in order to analyze micro-mechanics and detailed damage mechanics of trabecular bone [30, 36]. The ability to model deformation at the level of individual trabecular struts has led to the use of micro-FE as the mechanical driver for bone remodeling prediction [41] where the local strain/strain energy field drives the remodeling algorithm.

Initial development of the micro-FE method used images of in vitro specimens. With the development of peripheral quantitative computed tomography (pQCT), micro-FE has now been applied to in vivo studies [6, 49, 50].

15.1.4 Sensitivity Analysis

Sensitivity analysis is the process of establishing how sensitive the outputs of a model are to various inputs or settings [1]. This is done by varying the input within a range considered reasonable or realistic, and measuring the effect on the model outputs and on any conclusions drawn from model comparisons. A sensitivity test will give information on how precise the value of a parameter should be but will not show how accurate it is.

For the trabecular bone models discussed in this chapter, the assumptions which could introduce errors into the solution can be grouped as follows.

1. Digital representation: the accuracy with which the imaging modality represents the real bone.
2. Geometry and mesh generation: the accuracy with which the source image is segmented and the bone geometry is represented by the mesh.
3. Mesh quality: the numerical effect of element size, element shape and order of integration.
4. Material model: the accuracy with which the material model represents the material mechanical behavior.
5. Boundary conditions and constraints: the effect of assumptions made about behavior at the model boundaries.
6. Loading regime: accuracy of representation of the load in the simulated scenario.

Both the geometry (2) and the material model (4) are central to the development of a specimen-specific model and can be dependent on the source image.

In contrast, the boundary conditions (5) and loads (6) are usually independent of the source image and aim to replicate some in vivo or in vitro scenario. This chapter will review the effect of boundary condition choices but not that of loading cases.

The finite element solution depends in the mesh quality (3). A mesh sensitivity analysis is one of the fundamental verification steps highlighted in any course on finite element analysis. The choice of element type in any finite element model is not always clear cut. In solid models, the common types are linear or higher order elements of tetrahedral or hexahedral shape. There is often a balance between using a higher order integration function, which in some cases will converge with fewer elements but have more integration points (and hence a higher computational cost) and a linear option where a larger number of elements may be needed to reach convergence.

Sections 15.2 and 15.3 give some details of the methodology employed for micro-FE and continuum-FE respectively, along with evidence of sensitivity of key outputs to the assumptions detailed above. Although the image resolution is mentioned in the context of image segmentation, digital representation (1) is otherwise neglected. The bone material model (4) is assumed throughout the chapter to follow an isotropic Hookean elastic behavior. The effect of using a, possibly more accurate, nonlinear and/or anisotropic material model is not considered in this work.

15.2 Micro-FE Models of Trabecular Bone

There are two main methods to create micro-FE meshes from images. The first method requires a triangulation of the surface that first needs to be extracted from the images [13, 35]. The triangulated surface can then be filled with tetrahedral elements. The second one, referred to as the voxel-based method, creates the elements by converting the images voxels into hexahedral elements [47, 51]. This second

method can be used either to directly create hexahedra from voxels or to create hexahedral meshes that are mass-compensated [47]. Indeed, direct conversion of voxels to hexahedra can lead to loss of connectivity. These disconnected elements are not an active part of the model and are thus disregarded by any computation method. This induces a loss of bone mass compared to the actual bone mass of the specimen. The mass-compensated method accounts for this loss of connectivity and adds mass by artificially thickening the remaining bone trabeculae.

The voxel-based method is straightforward; however, if not smoothed, it produces jagged surfaces and edges, known as a staircase artifact, and thus is not accurate at the boundaries.

The meshes produced by a surface extraction method are smoother than voxel-based meshes; however, tetrahedral elements do not perform as well as hexahedral elements of the same order from a computational point of view [10, 39, 46].

When used in a small strain analysis with uniform elastic properties, the voxel-based meshes (using 8-noded elements) are particularly efficient as all elements are the same (same fixed orientation and shape), allowing an elementary tangent operator to represent the entire linear system [40, 52]. In this case, models with millions of degrees-of-freedom can be resolved on standard desktop computers.

15.2.1 Sensitivity to Imaging and Material Property Assignment

Before 3D CT images are converted into micro-FE models, they are usually binarized by thresholding, segmenting marrow and bone. The threshold level and method influence the results of micro-FE models as they influence the mesh and lose information on the partial volume voxels (voxels representing both bone and marrow). Another method of producing the micro-FE models is to directly convert the grey level into equivalent mechanical properties, thus accounting in the model for both bone and marrow (and partial volume voxels). The greyvalue to mechanical properties relationship thus influences the micro-FE results.

15.2.1.1 Sensitivity to the Threshold

The image threshold levels and the threshold method are two of the key points affecting the model behavior. They determine whether a voxel is represented or not as a solid element in the model. The threshold method thus has a direct influence on the bone volume modeled, as well as on the trabecular thickness and trabecular connection. Changes in these three parameters affect the apparent behavior of a trabecular model, since a high bone mass sample will be stiffer than a low bone mass one of the same size. Equally, local behavior will be affected. For example thin trabeculae are more likely to fracture and unconnected trabeculae do not participate in the weight bearing of the bone sample.

Table 15.1 Deviation of structural parameters for a 0.5% increase in threshold level; data from [20]

Deviation in	Low volume fraction samples (<0.15) (%)	High volume fraction samples (>0.2) (%)
BV/TV	5	2
Tb.Th	<3	<3
Computed apparent stiffness	9	3

Early on in the introduction of micro-FE models, the effect of the threshold method was analyzed. By comparing the behavior of human trabecular bone models at different image resolutions [47], it was shown that the use of a direct voxel conversion produces good results for high resolution models but not for lower resolution ones (with however a better apparent behavior representation than the local behavior one). The use of a mass compensated method produces more accurate results on an apparent point of view, however it compensates the loss of connectivity by a thickening of the remaining structure and thus significantly changes the micro architecture, and the local behavior.

The threshold level used for trabecular bone is also significant. Manual thresholding by different users leads to different results. Even though there is a low inter-user variability (0.5% difference in threshold value) to produce a “judged as optimal” threshold [20], the change in structural parameters extracted within that variability can be significant (see Table 15.1). It has been shown [4] that visual thresholding usually under-estimates the bone volume. Due mainly to the difference in the thickness of the trabeculae, the sensitivity of a visual threshold is lower for high volume fraction samples [4]. It is likely that the error is systematic per user [20]. This systematic error would therefore not be an issue for a comparative study performed by a single user as differences between groups could be detected anyway. It cannot however be blindly used to extract absolute quantitative mechanical parameters. Choosing a threshold value that accounts for an experimentally measured BV/TV (e.g. measured with Archimedes’ principle) would reduce the errors associated to manual thresholding. However, such an experimental value can prove difficult to measure. Indeed, the specimen whose density is measured using Archimedes’ principle needs to be completely immersed into distilled water, or another submersion liquid of known density, and degassed to remove all trapped air [16]. The measured density thus depends on the reliability of the degassing phase which is not easy to assess.

It should be pointed out that these different studies [4, 20, 47] did not account for geometrical nonlinearities that could occur even at low apparent strains. Their conclusions over the representation of mechanical parameters are thus valid only under a small strain hypothesis.

15.2.1.2 Sensitivity to the Relationship Used

Most micro-FE models of trabecular bone consider a homogeneous tissue-level bone modulus. However, the tissue modulus is dependent on the mineralization and thus can vary both within a trabecula and between struts [29]. Using a density-dependent modulus can thus account for the mineral content but also for the partial volume effects at the trabecular surfaces. This partial volume effect is caused by the error in capturing the surface of the trabeculae. Depending on the threshold value, voxels representing a mix of bone tissue and air or marrow can be considered as being 100% bone or 100% air/marrow. The material properties of those areas are thus either over-estimated or under-estimated. Using material properties function of a local greyscale rather than homogeneous values after thresholding can thus help to reduce the sensitivity of the model to the threshold. With a non-linear relationship, Homminga et al. [25] showed that using a greyscale-based modulus value for each voxel instead of a homogeneous value reduces the mean deviation and the range of deviation of the computed apparent elastic modulus from the experimental apparent elastic modulus. Bourne et al. [5], proposed a linear relationship between the X-ray attenuation and tissue modulus. This relationship assumes a modulus of 20 GPa for a tissue of 1.1 g/cc. Using different slopes for the linear relationship, they found a slope of 1.4 most precisely predicted experimental modulus. They demonstrated the apparent elastic modulus value for a homogeneous 20 GPa model was significantly greater than for all types of inhomogeneous models. Following the same principle, Harrison et al. [21] calibrated their linear relationship with micro-indentation tests. Finally, a more complex relationship accounting for the mineral content of the bone was proposed by Bourne et al. [5]. They defined a theoretical relationship relating micro-CT mineral density to tissue density and elastic modulus. The derivation uses prior knowledge of the bone constituents' volume fractions and individual constituent densities to calculate the volume and mass of each constituent within a voxel.

15.2.2 Sensitivity to the Finite Element Mesh

To perform a finite element analysis on processed images, the geometry they represent needs to be discretized into a finite element mesh. A finite number of geometrically simple elements (such as hexahedra and tetrahedra) is used to represent the potentially very complex geometry represented in the images. The mesh built on the processed images is the next source of errors to which the results are very sensitive. The element size needs to be appropriate so that the geometrical discretization is accurate. However, a series of numerical errors occurs depending on the element size, type, and integration method. The sensitivity of the results to these types of errors is overviewed here.

15.2.2.1 Sensitivity to the Finite Element Mesh Size

Early work on the influence of element size [31] showed that computing an apparent stiffness with a linear model and a voxel-based mesh produced results which were very sensitive to the mesh resolution. However, the image resolution those meshes were built from (given the trabeculae are properly resolved) did not seem to play an important role. Low density samples seemed more sensitive to the mesh resolution than high density ones. Convergence studies for a fully linear model and a voxel-based mesh [19] have shown that the element size should be less than one fourth of the trabecular thickness. No convergence studies for meshes built on triangulated surfaces of trabecular structures were however found in the literature. This gap is partially covered hereafter.

Micro-CT images of the trabecular core of a bone antler [13] were used to analyze several sensitivity aspects of micro-FE models. It consisted of a 2.11 mm cubic specimen (BV/TV of 10.88 %), imaged at a cubic voxel size of 8.64 μm (see Fig. 15.1a). Ten triangulation surface meshes obtained with a surface reconstruction algorithm [13] were constructed at different resolutions (producing from 65,000 to 120,000 triangles). Linear tetrahedral meshes built on those surface triangulations (i.e. meshes with 130,000–290,000 elements) were used to analyze the effect of mesh size on a finite strain model of compression tests. The material at trabecular level was considered as following an isotropic Hookean elastic behavior, described with a Young's modulus of 7.78 GPa [14], and a Poisson's ratio of 0.3. The performance of those meshes was evaluated by comparing the computed apparent stiffness (computed with a linear regression at 0.2 % compression), and the force level for 5 % compression tests in each direction. The finite strains micro-FE models were solved using the non-linear object-oriented implicit software Metafor (LTAS-MN²L, University of Liège, Belgium).

The coarser meshes show places (highlighted in red on Fig. 15.2) where only one element spans across the trabecular thickness. The convergence study shows (Fig. 15.3) that both the apparent stiffness and the maximal force decrease when increasing the number of elements. The apparent stiffness decreases by 6.2 % from the coarser mesh to the finer ones, while the maximal force decreases by 10.4 %.

15.2.2.2 Sensitivity to Type of Finite Element

The performance of a model is not only sensitive to the mesh resolution but also to the shape of each element. Early studies on the subject [47] showed that for a fully linear elastic model, there were no significant differences between the performances of a mass-compensated linear hexahedral mesh and a tetrahedral one. As soon as geometrical nonlinearities are included in a model, those conclusions may no longer be valid. To analyze the element shape influence on a model performance, the bone antler sample introduced previously was meshed using three different algorithms. The first one used a surface-reconstruction algorithm as presented in Fig. 15.2 (we use here the finest mesh from that study), thus producing a smooth tetrahedral mesh; the

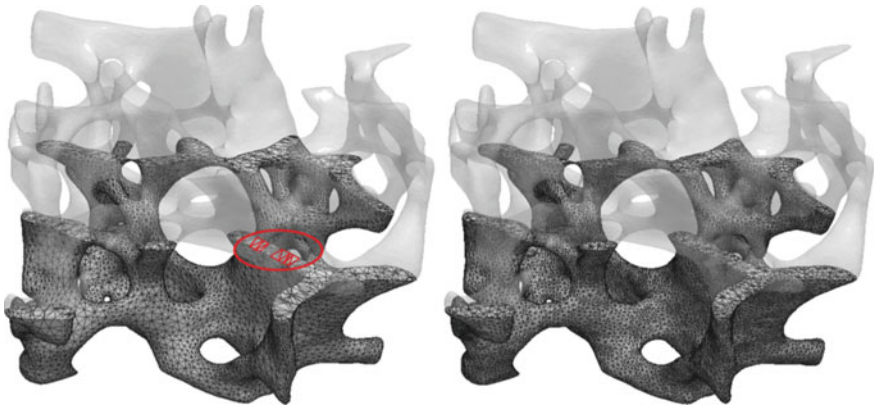
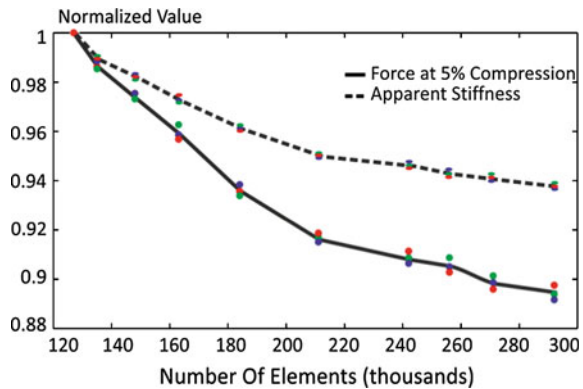


Fig. 15.2 Cut through antler meshes. *Left* 130,000 elements mesh, *Right* 290,000 elements mesh

Fig. 15.3 Convergence study—normalized values for compression tests in three directions (*color dots*): stiffness (*dashed line*) and force (*plain line*) (*color online*)



second one used a direct voxel conversion algorithm, thus producing a jagged hexahedral mesh (see Fig. 15.1b); the third one used a direct voxel conversion followed by a topology-preserving smoothing algorithm [12], producing a smooth hexahedral mesh. Two meshes were produced using this last method, the first one involved one smoothing iteration, the second one two smoothing iterations. The performance of these four meshes was evaluated comparing the computed apparent stiffness (computed with a linear regression at 0.2% compression), the maximal force level, and the deformed micro-structure for 10% compression tests in each direction, using the same material model as earlier.

Even though the smoothing algorithm preserves the initial topology as accurately as possible, some shrinkage is inevitable. The bone volume represented by each mesh is slightly different (Table 15.2). Smooth hexahedral meshes represent a smaller bone volume than the voxel-based mesh, the tetrahedral mesh represents however a similar bone volume. The computed apparent stiffness slightly decreases with smoothing in the hexahedral meshes. The computed force (Fig. 15.4) is equivalent for the three

Table 15.2 Mesh type dependent parameters

Relative difference (in % of the voxel mesh value)	Smooth hexahedral mesh (1 smoothing iteration)	Smooth hexahedral mesh (2 smoothing iterations)	Tetrahedral mesh
Volume	-4.32	-7.89	+0.75
Stiffness	-3.71 (± 1.72)	-5.55 (± 0.52)	+39.63 (± 7.05)

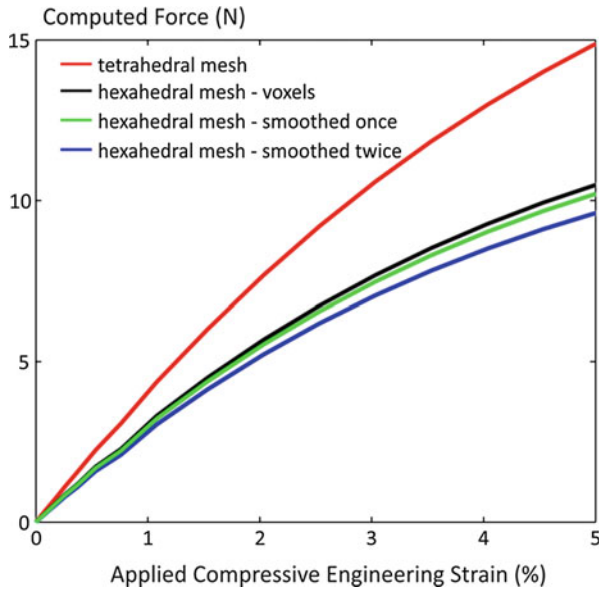


Fig. 15.4 Example of force versus applied engineering strain function of the element type

hexahedral meshes, slightly decreasing as the smoothing increases. The tetrahedral mesh requires however a higher force to be applied, especially at large strains.

Finally, the deformation pattern between the hexahedral meshes shows only slight differences while that of the tetrahedral mesh is completely different (Fig. 15.5). In particular, direction of trabecular bending can be opposite.

It is thus clear that the choice of element shape for a given mesh resolution influences not only the local behavior of the model but also its apparent behavior. A thorough comparison with experimental data on both the apparent and local level is needed to fully evaluate the best choice of element type. It should finally be pointed out that the conclusions addressed here are only valid on a sample with low BV/TV and considered as following an isotropic Hookean elastic behavior. Differences in results for the force level or the deformation pattern may be different for other types of material behavior more appropriate to model bone trabeculae at large strains.

For a given element shape and size, the chosen integration method will affect the integration results. Geometrical discretization errors lead generally to softening

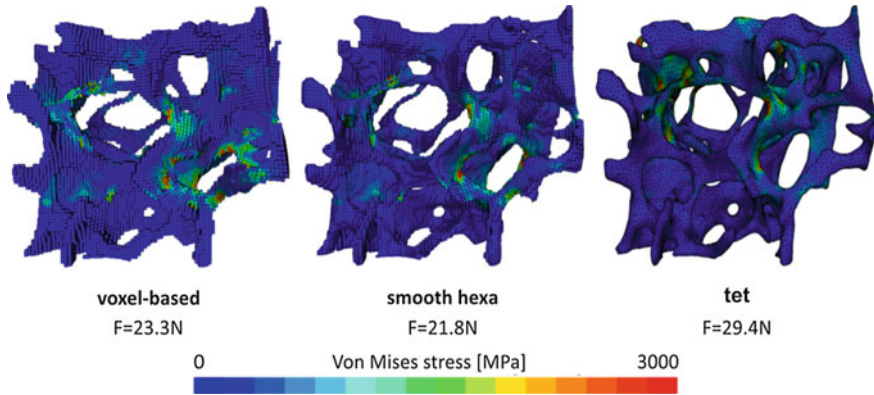


Fig. 15.5 von Mises equivalent stress fields and values of the applied force at 10% applied engineering strains

(due to an underestimation of the volume at the threshold and the meshing phases). For hexahedral elements in a linear integration (8 integration points), there can be a stiffening effect due to shear locking if elements happen to be submitted to pure bending. In a finite element solution process the stress field, and all other secondary fields, are computed accurately at the integration points, and reducing their number reduces the accuracy of the stress field. A reduced integration (one integration point) avoids shear-locking but degrades the computed stress field. Quadratic integration (27 integration points) also avoids shear locking and does not degrade the secondary fields (as the number of integration points increases). It thus can be used even at low resolutions for accurate stress fields. The main disadvantages of a quadratic integration are the increase in computational cost and the increase in sensitivity in inaccurate geometry (such as staircase artifacts). The opposite behavior between geometrical discretization softening and integration stiffening explains [13] why 8-noded hexahedra, using a sufficient resolution, are accurate concerning the computation of global apparent values in small strains analysis. For a quadratic integration however, as discretization errors are not compensated by integration errors, the computed apparent values are less accurate than 8-noded hexahedra (even though both results are strongly correlated).

15.2.2.3 Discussion

A number of studies have been performed on the analysis of hexahedral mesh performances representing trabecular bone microstructure. However voxel-based meshes, while straightforward to build, do not represent the trabecular surface accurately as they produce jagged edges. Tetrahedral meshes allow the representation of smooth surfaces more easily. There are few convergence studies on the performance of tetrahedral meshes representing trabecular microstructure. The current work illustrated

that the mesh has to be fine enough in order for more than one element to span across the trabecular thickness. However, drawing a definite conclusion on the number of elements needed over the trabecular thickness is difficult. Indeed as all elements do not have the same size, measuring the quality of the mesh by the ratio of the mean edge length to the mean trabecular thickness is not representative of the mesh quality. For the presented meshes, that ratio indeed varies from 3.04 to 3.47 when increasing the number of elements. Looking at that ratio only would thus not highlight the differences observed between meshes. Only a local inspection of the mesh can help determine whether or not the mesh is fine enough.

Another method for avoiding jagged surfaces is to smooth out voxel-based meshes, thus obtaining smooth hexahedral meshes. This smoothing operation has to be done with as little volume loss as possible. The performance of smooth hexahedral meshes was compared to that of a voxel-based mesh and a tetrahedral mesh, showing differences in computed force and stiffness. The stiffness and force decrease of the hexahedral meshes can be explained by the proportional volume loss. The tetrahedral mesh shows higher apparent stiffness and force that cannot be explained by the small volume increase. The difference is most probably due to the numerical stiffness of the linear tetrahedron. Indeed, the linear tetrahedron (1 integration point) is known to be stiff while the hexahedra are here integrated on 8 nodes with selective reduced integration to reduce shear-locking effects. The increased apparent stiffness behavior of the tetrahedral model is therefore most likely to be a numerical artifact. This numerical stiffness is less present in second (or higher) order tetrahedra. However, due to their simplicity and robustness, elements with linear shape functions are often preferred for non-linear problems, particularly when these involve large strains, frictional contact or material nonlinearities.

15.2.3 Sensitivity to Boundary Conditions

This section discusses the sensitivity of micro-FE models to the representation of boundary conditions. Boundary conditions represent experimental loading and support conditions of the modeled specimens. When qualitatively comparing the performance of several models, the applied boundary conditions might not be of importance to extract differences or similitudes between different groups as long as they are applied in the same way for each group. When quantitatively comparing models and experimental data, the accuracy of the boundary condition representation can be of great importance.

Most experimental tests of trabecular structure are compression tests of cylindrical samples. Representing the experimental setup in details can be considered. The interaction between the bone sample and the experimental setup (the sample extremities can be embedded into end-caps) is however often unknown. The setup is thus often simplified into a fixed end, on top of which lays the sample, and a moving one, compressing it. The applied boundary conditions can allow either for the material to move in the plane perpendicular to the loading direction (free boundary condition)

or not (constrained boundary conditions). Several studies have shown the influence of model choice on the results. The models are highly sensitive to the representation of the gripped end by constrained or free boundary conditions. Apparent parameters such as the apparent stiffness can show variations up to 40% [31], with a constrained numerical setup stiffer than a free one. Note however that a compression experiment with or without end-caps can show comparable deviations [28]. Using micro-FE models coupled to an optimization method to compute the hard tissue modulus gives however results which are better correlated [26] when the samples are tested with end-caps and modeled with constrained BC's, than tested without end-caps and modeled with frictionless contact conditions or free moving boundaries. The difference may be due to the fact that modeling a free moving boundary with frictionless behavior is not fully representative of the experimental conditions as purely frictionless behavior is not obtained. Approximating the boundary conditions usually leads to a higher tissue modulus than representing the actual experimental setup [4]. The method used to represent constrained or free boundary conditions can still be achieved in different ways using for instance either nodal constraints or contact conditions.

To analyze the effect of boundary representations, the bone antler sample introduced previously was compressed using eight different boundary setups (Fig. 15.6), all representing a fixed bottom surface and a moving upper one. Four of those setups had constrained boundary conditions at each end (Fig. 15.6a–d) and four had free boundary conditions at each end (Fig. 15.6e–h). The constrained condition on the fixed surface was represented either as a node constraint (cases a and b), for which the surface nodes were pinned in 3D, or as a friction contact with a rigid plane (cases c and d) using a friction coefficient of $\mu = 0.8$. The constrained condition on the

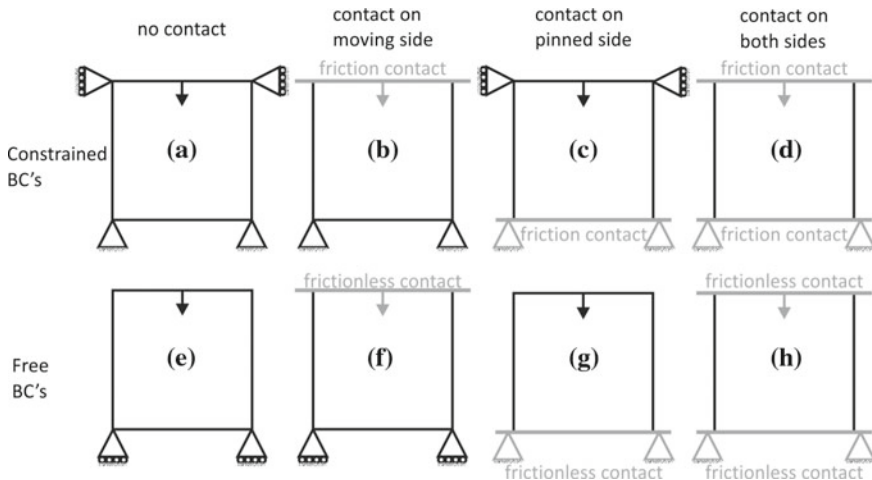


Fig. 15.6 Different types of constrained (*top row*) and free (*bottom row*) boundary conditions for a vertical displacement. Constraints in *grey* are applied to contact planes; constraints in *black* are applied to surface nodes

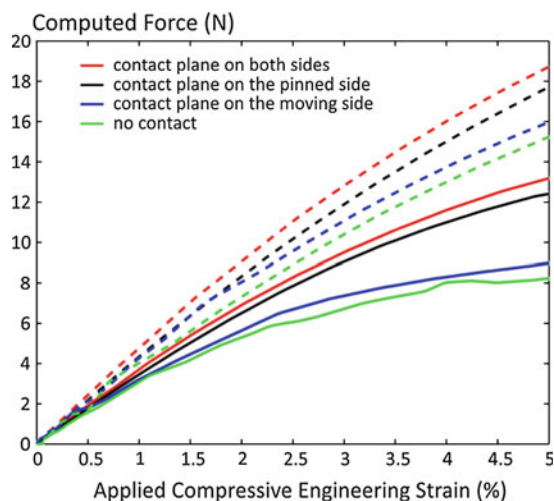
Table 15.3 Boundary conditions type dependent parameters (values in parentheses are the standard deviations)

Relative difference in stiffness (in % of the “no contact” stiffness)	Contact on moving side	Contact on pinned side	Contact on both sides
Constrained type BC’s	51.3 (±19.4)	76.9 (±23.5)	86.8 (±15.4)
Free type BC’s	26.8 (±3.5)	34.5 (±10.5)	51.3 (±9.4)

moving surface was similarly represented either as a node constraint (cases a and c) or as a contact condition (cases b and d). Similarly the free condition on the fixed surface was represented either as a node constraint (cases e and f), for which the nodes were pinned in the directions perpendicular to the compression, or as a frictionless contact condition (cases g and h). The free condition on the moving surface was either a node constraint (cases e and g) or a frictionless contact condition (cases f and h). For the case where two frictionless contact conditions were used (case h) the central node of the bottom surface was pinned to avoid rigid body motion.

As previously a compression of 5% was applied in a large strains framework and the performance of each model was assessed comparing the computed apparent stiffness and the maximal force reached. Exactly as constrained BC’s are stiffer than free ones, contact BC’s are stiffer than node constraints, whether constrained or free (Table 15.3). The deviation in the force between the different free representations stay proportional with the level of compression while the constrained representation shows increasing deviation with compression (Fig. 15.7).

Fig. 15.7 Example of force versus engineering strain function of the BC type (plain lines free BC’s, dashed lines constrained BC’s)



The ability to move laterally while applying a compression allows the virtual setup to be more compliant. The computed apparent stiffness and force decreases with the increasing flexibility for the sample to move or expand laterally.

15.3 Continuum Level Models of Trabecular Bone

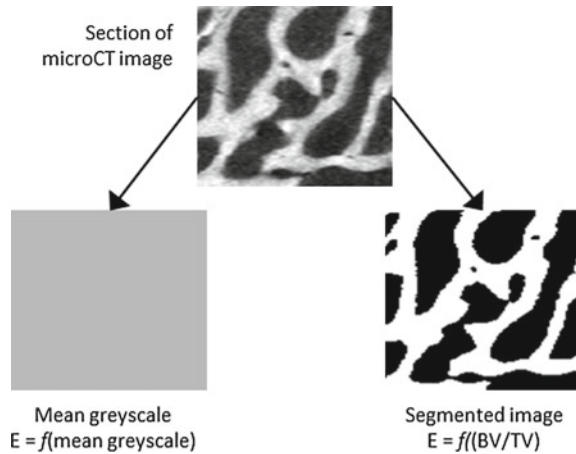
Finite element models of trabecular bone at the continuum level have existed for many decades and have been used to investigate a range of clinical situations. Whilst micro-FE models have become more prevalent for the simulation of small regions of trabecular bone, the computational cost can be prohibitive, and whole bones and joints are still routinely simulated at the continuum level. Advances in imaging technologies such as CT and micro-CT have enabled more information to be derived for the generation of such models, including both the geometry and the spatially varying material properties.

15.3.1 *Sensitivity to Imaging and Material Property Assignment*

Continuum-level finite element models of bones with inhomogeneous material properties based on the underlying bone density have become widely adopted, and have been shown to provide better agreement with experimental data than those using uniform properties [44]. The elastic modulus of elements representing the trabecular bone regions within these models are often assigned on an element-by-element basis. Two approaches are commonly used to derive the elastic modulus values, as illustrated in Fig. 15.8. In the first (the ‘greyscale’ approach), an average greyscale is calculated from the voxels within the element volume, and the elastic modulus is calculated as a function of this value.

In the second (the ‘segmentation’ or ‘BV/TV’ approach), the underlying image is first segmented in order to calculate the bone volume fraction (BV/TV) and the modulus is then calculated as a function of the BV/TV. The segmentation approach allows extracting further information on the microstructure. In particular, information about the anisotropic organization of trabeculae can be computed from the segmented images. In that case, fabric tensor based orthotropic material properties can be derived. Accounting for anisotropy showed it can improve the correlation of bone morphology to bone strength for several anatomical sites [32, 37].

Fig. 15.8 Example of two different approaches for the derivation of mechanical properties from the micro-CT image data. For each element within the model, the elastic modulus is calculated based on either the mean greyscale (greyscale approach) or the BV/TV (segmentation approach) of that region



15.3.1.1 Sensitivity to the Methodology Used

In order to examine the sensitivity to the approach used, models from two previous specimen-specific studies [45, 54] were examined using both methods. In total, ten vertebral bodies (four human and six porcine) were imaged using micro-CT at a cubic voxel size of 0.074 mm, and tested under axial compression. From the micro-CT scans, two models were built of each specimen with the same element size of 1 mm. In one model, the greyscale approach was used, with the modulus linearly related to the mean greyscale of the voxels within the element. In the other, the segmentation approach was used, by first segmenting the images with a species-specific threshold (i.e. different for the human and porcine specimens). The elastic modulus was then linearly related to BV/TV. In both cases, the relationship between the image data and elastic modulus was optimized until the average error between the predicted stiffness of the models and the experimental values was minimized. The resulting predictions were compared to the experimental values and are shown in Fig. 15.9. The absolute average errors in stiffness for the two sets of models compared to the experimental results were then calculated. It was found that these errors were very similar for the two methods (6.5% for BV/TV method and 8.3% for greyscale method). Since the experimental error is likely to be of a similar order of magnitude to these errors, the results suggest that there is no advantage in using one method over the other, providing that the parameters used have been optimized.

15.3.1.2 Sensitivity to the Threshold for the Segmentation Method

As discussed in Sect. 15.2.1.1, the threshold selected to segment an image into trabecular bone and trabecular space will affect the thickness of the trabeculae and it has been shown that the choice of threshold can have a considerable effect on the

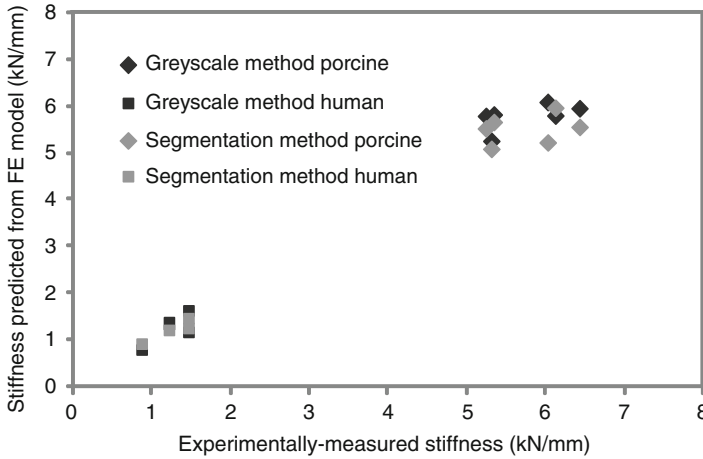


Fig. 15.9 Agreement between FE model predictions and experimental stiffness values for ten porcine and human vertebrae modeled using element-specific material properties based on BV/TV and mean greyscale data derived from the micro-CT image data of the specimens

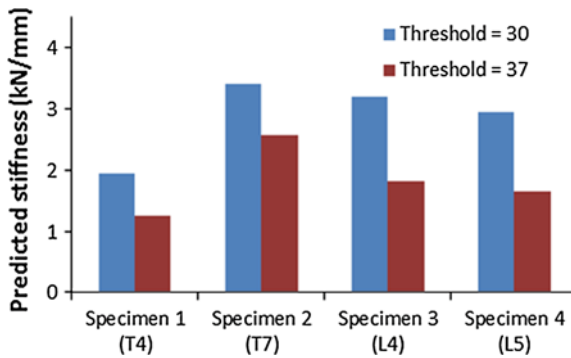


Fig. 15.10 Predicted stiffness of four FE models of human vertebra [54] generated using the segmentation method to assign element-specific elastic modulus values. For each specimen, the predicted stiffness when two different threshold values were used to calculate the BV/TV is shown

calculated BV/TV values [38]. This then has a knock-on effect on the resulting FE model stiffness, as is illustrated in Fig. 15.10 for the four models of cadaveric vertebrae described above [54]. Here, two threshold values were selected to represent extremes of the range likely to be picked ‘by eye’, and it was found that the predicted stiffness varied by a mean of over 30%.

15.3.1.3 Sensitivity to the Relationship Used

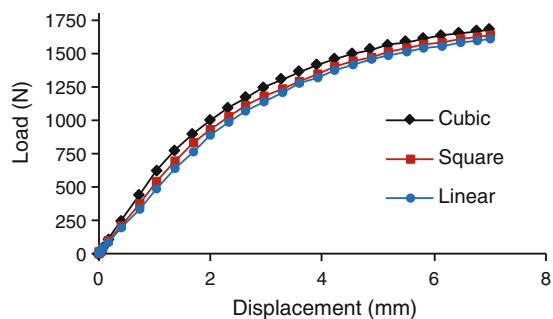
Whichever method is used to determine the elastic modulus or other material properties from the underlying image data, the relationship between the greyscale and the property will have an effect on the final model. A number of different relationships have been used for both the BV/TV and the greyscale methods. Many of these relationships originate from density-modulus equations derived from previous experimental tests on trabecular bone specimens. The number of available equations in the literature is large, and several studies have investigated the sensitivity of the model outputs to the equation used, in many cases making direct comparisons with experimental tests in order to determine the most suitable relationship (e.g. [2, 11, 17]). These studies have generally found that the FE model predictions of apparent stiffness and local strain are highly sensitive to the equation adopted, which is unsurprising when the range of different equations in the literature is considered. However, there is little consensus across the studies on a single ‘optimum’ equation and, even within studies, different equations appear to fit different individual specimens better (e.g. [2, 17]). Many of the equations used are based on a power-law relationship between a measure of bone density (ρ) (ash density, apparent density, BV/TV etc.) and elastic modulus (E):

$$E = a\rho^b$$

The relationship derived by Morgan et al. [34] with a relatively low power ($b = 1.49$) appears to commonly be amongst the closest when the resulting FE models are compared to experimental data [11, 17]. In the study by Cong et al. [11], the authors determined optimum values of a and b to best fit the stiffness predictions of the FE models of femora to results obtained experimentally. They found an even lower power ($b = 1.16$) obtained the best results from a power-law equation. In another study [54], it was found that the value of the power had little effect on the performance of an individual model of a spinal vertebra, providing the associated constant, a , was optimized, as can be seen in Fig. 15.11.

The effect of the power will depend on the spread of the greyscale values within the underlying images. Extremely bright and dark regions in the image, which may

Fig. 15.11 Load–displacement curves for a vertebral model generated using different relationships. Adapted from [54]



be caused by artifacts, will dominate the model behavior with higher power terms by causing regions of overly large or small modulus values. The low sensitivity seen here makes a linear relationship a reasonable choice for this study. However the sensitivity may be affected by bone density range within the specimen set.

15.3.1.4 Discussion

A number of different methods have been used to both extract information from three dimensional image data sets and to derive finite element mechanical properties from this information. Two common methods for extraction, described here as the 'greyscale' method and the 'segmentation' method appear to yield models with relatively similar levels of accuracy. Both have their advantages and disadvantages. The segmentation method is sensitive to threshold, which in turn is sensitive to the scanner and settings used. Use of phantoms and/or automatic segmentation methods could allow scans from different imaging systems to be used, but as yet, little work has been undertaken to develop a robust framework for this process. The greyscale method is dependent on both the scanner and its settings, as well as the material within the marrow space. The use of phantoms is common place to calibrate scanners and relate the greyscale to the bone density. However, the greyscale of the trabecular space will be very different for dry bone specimens compared to those where the marrow is intact. So, whilst phantoms may get around some of the problems of using different scanners, it is more difficult to take account of different materials within the trabecular space.

The model predictions have been shown to be sensitive to the relationships used to assign the properties from this image information. The literature is awash with different equations and there is no clear consensus on an optimum choice. For applications with a limited density range, it may be possible to use a simple linear relationship, provided that the terms in the equation can be tuned for the specific species and type of bone that is used.

15.3.2 Sensitivity to the Finite Element Mesh

15.3.2.1 Sensitivity to the Finite Element Mesh Size

Many factors affect the convergence behavior with respect to the elements size of a finite element model, and the inhomogeneous properties, often coupled with a complex geometry, add particular challenges to the analysis of bone. To isolate the effects of material properties from those of the geometry, a study was undertaken where six rectangular cores of bone were extracted from continuum-level models of whole vertebrae and examined in isolation [27]. As the mesh density was altered (Fig. 15.12), models where the bone properties were inhomogeneous, and based on the underlying image greyscale, displayed less consistent convergence than those

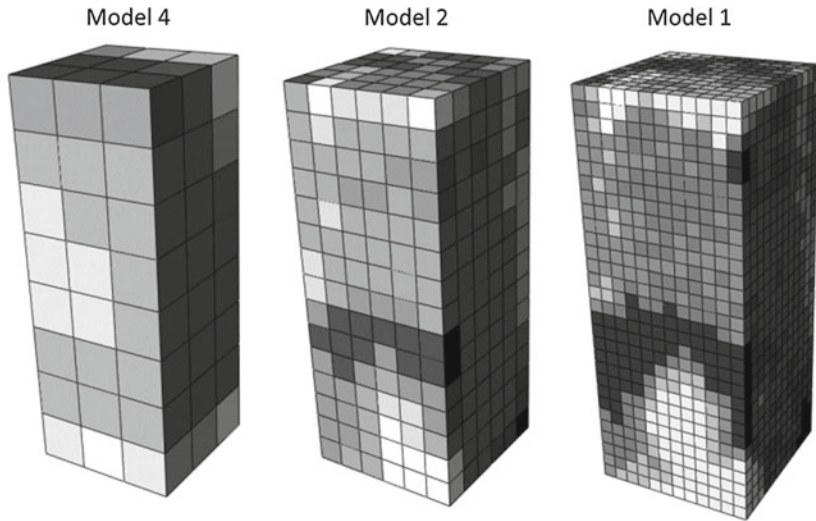


Fig. 15.12 A typical cuboid ($12 \times 12 \times 32 \text{ mm}^3$) of trabecular bone meshed with three different element sizes (Model 4 = 4 mm^3 , Model 2 = 2 mm^3 , Model 1 = 1 mm^3). Adapted from [27]

Table 15.4 Difference in predicted stiffness between homogenous and greyscale-based FE models of trabecular bone cores generated with different element sizes (Model 4 = 4 mm, Model 2 = 2 mm, Model 1 = 1 mm)

	Homogenous properties	Greyscale-based properties
(Model 4-Model 2)/Model 2 (%)	6.3	5.5 (± 4.3)
(Model 2-Model 1)/Model 1 (%)	0.030	3.8 (± 2.5)

From [27]

where the properties were homogenous (Table 15.4). This is not surprising, since within the inhomogeneous greyscale-based models element size will alter not only the number of degrees of freedom, but also the distribution of material properties.

Zhao [56] decoupled these two effects by generating models of synthetic trabecular bone specimens based on micro-CT images in two different ways. In the first method, the images were down-sampled to different resolutions using a method incorporating partial volume effects. Then finite element models were generated with elements of the same size as the down-sampled images resolutions. In the second method, the images were down-sampled to the coarsest level, and then finite element models created from the images with varying mesh sizes, such that there were different numbers of elements but the materials properties of each were based on the same underlying greyscale grid (Fig. 15.13). Where this latter method was used, there was a rapid convergence that remained as the element size decreased. However with the first method, there was some evidence of convergence at larger element sizes (where the element was much larger than the trabecular bone structure), but as the image

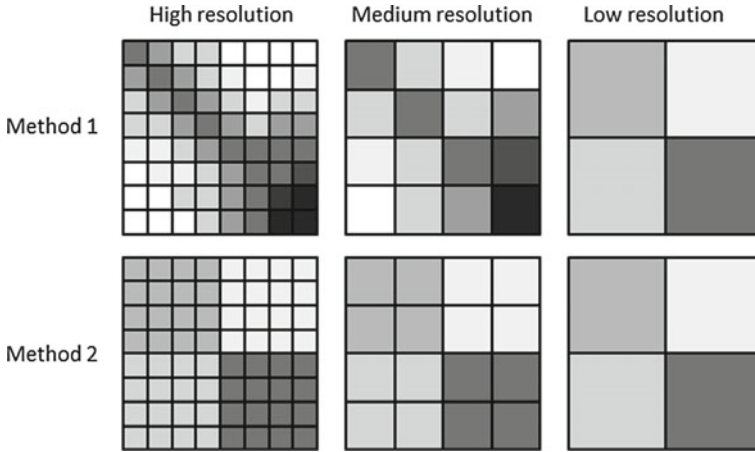


Fig. 15.13 Example in 2D of two methods of generating FE models from images at different element sizes. In Method 1, the underlying image is down-sampled, and the elements are assigned properties based on the image greyscale at that down-sampled level. In Method 2, the images are first down-sampled to the lowest resolution, then meshes of different sizes are used, such that the properties are always based on the same down-sampled image. Adapted from [56]

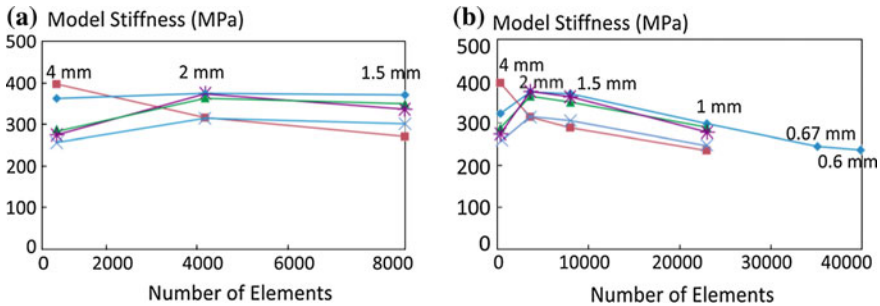


Fig. 15.14 Results of mesh convergence tests using **a** Method 1 and **b** Method 2 for models generated from images of a synthetic trabecular-like structure. Each line depicts the results of a different image data set. In Method 2, as the element size is decreased, the elements become a similar size to the trabeculae (~1 mm in this case) and eventually a second convergence occurs once the model becomes a micro-FE model. From [56]

resolution neared that of the trabecular structure itself, there was instability, since the elements were beginning to represent either trabecular space, or trabecular bone, rather than an average of the two (Fig. 15.14).

In a study including both isotropic and orthotropic models of cylindrical samples of deer antlers and other cellular materials, Mengoni et al. [33] decoupled the mesh size effects from the region size from which the material properties are extracted. The samples were meshed at a given fine resolution while the image-based material properties were extracted on regions of different size, assigning the same set of

properties to the underlying cluster of mesh elements. This method showed evidence of convergence for decreasing size of element clusters, before reaching the element-by-element level. For a given mesh size, while assigning material properties on an element-by-element basis may be necessary for isotropic models where only the modulus is evaluated from the image, for orthotropic models where fabric is also evaluated, it is less necessary and a cluster approach may be appropriate here because more information is extracted from the images.

15.3.2.2 Sensitivity to Type of Finite Element

There are relatively few studies that have specifically analyzed the element type in relation to continuum bone models. Ramos and Simoes [39] compared element type and order for simplified and realistic geometry femur models with homogeneous material properties. For the realistic model, the results for models with hexahedral elements converged with a lower number of elements than for the tetrahedral models, but there were some (<10%) differences between the first and second order converged results. For the tetrahedral elements, there was little difference in the results between the first and second order element types for the same number of elements. Their general conclusion was that the type of element “did not evidence significant differences”, however this will be very dependent on the nature of the problem and level of accuracy required. In the case of bone models with inhomogeneous, image-based material properties a change in element size will affect multiple aspects of the model (Sect. 15.3.2.1) and convergence testing is not straight forward.

15.3.3 Sensitivity to Boundary Conditions

The sensitivity of ovine trabecular bone models to the representation of boundary conditions replicating an experimental test were examined by Sikora [43]. Experimental tests were undertaken in which trabecular cores (approximately 10 mm in diameter and 20 mm in length) were extracted from ovine vertebrae, and set in delrin endcaps using a small quantity of polymethylmethacrylate (PMMA) cement, as shown in Fig. 15.15a. The specimens were imaged using an HR-pQCT (XtremeCT, Scanco Medical, Switzerland) with a voxel size of 0.041 mm and converted to finite element models with a 1 mm mesh size using proprietary software (ScanIP v4.2, Simpleware Ltd., UK). Four different methods of representing the boundary conditions on the bone were investigated. For each case, four specimens were investigated and the mean difference in predicted stiffness between the case representing the full experimental set up (Fig. 15.15a) and the different simplifications (Fig. 15.15b–d) were calculated.

The results are presented in Fig. 15.16. It can be seen that large relative differences on the stiffness occur where the boundary conditions do not provide the lateral

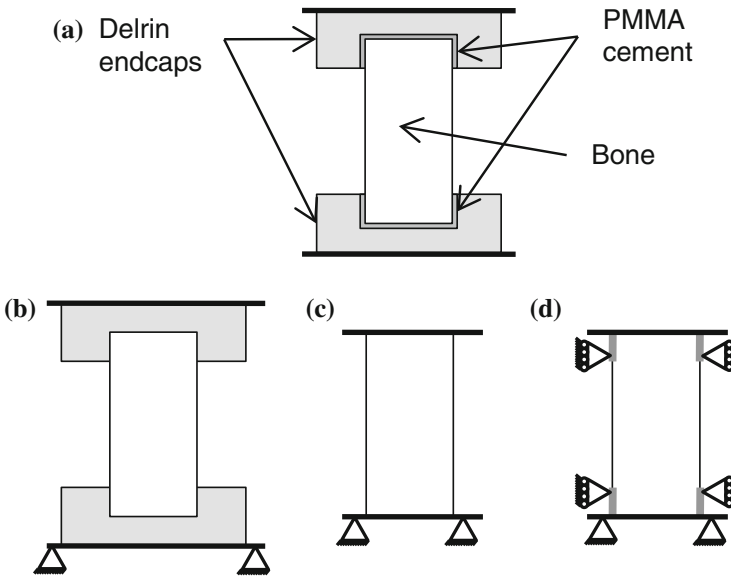


Fig. 15.15 Schematics of FE models of a trabecular bone compression test representing **a** the experimental set-up including the endcaps and PMMA cement, **b** a simplified version without the PMMA cement, **c** only the bone and **d** the bone with additional boundary conditions preventing lateral displacement (shown as *grey lines*). In all cases, the models were tied to rigid plates on the *top* and *bottom* surfaces. Adapted from [43]

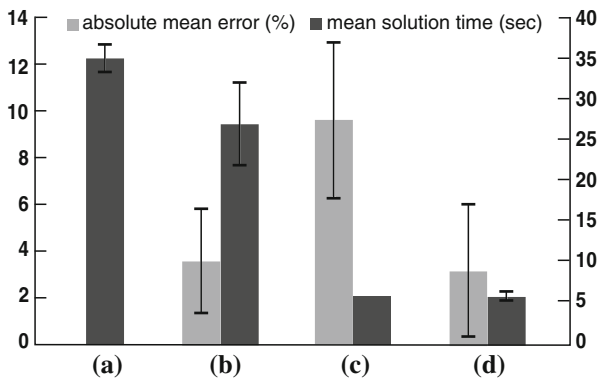


Fig. 15.16 Results for a boundary condition sensitivity study [43] undertaken on four models under the four different boundary conditions shown in Fig. 15.15. The absolute mean stiffness differences (*error bars* show standard deviations) are shown for cases (b)–(d) compared to the reference case (a). Mean solution times are also shown

constraint at the ends (case c). Similar results were also found by Zhao [56] using synthetic bone specimens. Here, an investigation was also undertaken to examine

the effects of different boundary conditions on a model similar to that shown in Fig. 15.15c.

The representation of whole bone specimens is just as sensitive to loading conditions, as was illustrated by Jones and Wilcox [27]. Here, specimen-specific models of spinal vertebrae were constructed to replicate an experimental compression test where the upper endplate was loaded via a steel ball, allowing it to tilt relative to the lower endplate. The predictions of stiffness from the FE models was found to be highly sensitive to the position at which the load was applied, with even deviations of 2 mm in location causing nearly 20 % change in the predicted stiffness. Such results illustrate not only the importance of boundary conditions in an FE model, but that this is also an issue with an experimental test, although it is often less apparent in the laboratory because of the variation between specimens.

From these results, it is clear that boundary conditions are important and changes in their implementation can cause substantial differences in model predictions. Even known conditions in a laboratory test can be represented in different ways, and simplifications can lead to substantial errors. The endcapped trabecular bone specimen should be very ‘easy’ to model and the situation becomes worse if the ends of the specimen are free to move laterally, as Zhao [56] showed, since the coefficient of friction between the bone and the loading platen is usually unknown. Where there are more unconstrained degrees of freedom, such as in the whole vertebra model, then the location of the constraints can play a major role and the replication of an experimental test becomes increasingly more difficult.

Boundary conditions are often applied without much justification, and these examples demonstrate that there is a need for thorough sensitivity tests since subtle changes in their application can lead to quite different results.

15.4 Discussion

This chapter provided evidence on the sensitivity of trabecular bone model outputs to the assumptions made during their construction, for micro-FE and continuum-FE models.

The level of sensitivity to several aspects, such as image segmentation and meshing, depended on the density of the specimen considered and the amount of deformation modeled. Model results were less sensitive to the assumptions made with the presence of higher density bone within the source specimen or with a low strain assumption during virtual testing. This is an important consideration when applying established methods to a new site in the body or new disease state.

15.4.1 Segmentation

Micro-FE predictions are sensitive to the threshold value used to segment the bone from the source image as this process affects both the total bone volume and can affect the connectivity within. Therefore changes to the threshold value will affect both macro behavior and that at an individual trabecular level. This sensitivity is more pronounced for low density bone specimens. The segmentation process also affects outcomes in the case of continuum-FE models which are based on BV/TV values. It is unclear whether one modeling approach provides a lower sensitivity to the image segmentation process as the available tests are not easily comparable (Sects. 15.2.1.1 and 15.3.2.1). In the absence of an ideal threshold value, the segmentation of the micro-structure should be as consistent as possible between specimens. The best chance of this consistency is through the use of phantoms, user training and automation where possible.

15.4.2 Meshing

The choice of optimum element type for micro-FE models is dependent on the intended application. For example, a direct conversion from image voxels to linear hexahedral elements may be a good choice where a linear analysis is sufficient, computational cost must be controlled and only macro level behavior is of interest. The representation of bending behavior of individual trabecular struts remains a challenge with each element shape and type of integration delivering different benefits and drawbacks (Sect. 15.2.2.3). Ultimately the choice for a particular project will likely be driven by the level of accuracy required and the computational resources available.

Regardless of what other sensitivity analyses are undertaken, a mesh convergence test is recommended for any new model or different application of an existing model [23]. However, the choice of element size for continuum-FE models is somewhat arbitrary. This chapter has discussed how the underlying structure, represented by the element-specific material properties, is captured at different resolutions depending on the element size. The image to material property conversion formula is likely dependent on the element size and therefore can be calibrated for a particular choice. The effect of element size is therefore corrected for during that calibration process. For lower resolution source images (such as traditional hospital grade QCT) the image resolution may provide a logical cap for the mesh resolution.

The choice of element integration for the representation of macro behavior using continuum-FE models requires the consideration of similar factors to the representation of micro behavior using micro-FE models. For example, care should be taken when using linear elements with standard integration if there is large deformation or bending, and a sensitivity test is always a useful check.

15.4.3 Image-to-Material Properties Relationship

Applying suitable material properties to finite element models of bone is challenging and there is currently no consensus on the optimal method. Although the use of source images provides a method of applying a realistic distribution of those properties, that distribution is reliant on the accuracy of the imaging modality and the choice of conversion formula. Relationships between image greyscale, density and material constants are sometimes derived from in vitro material tests, sometimes from theory and sometimes calibrated in silico against experimental data. Regardless the resulting material distribution is dependent on specimen preparation and scanner settings, underlining the importance of calibration phantoms during the image capture. In addition it is possible for any image to contain artifacts which will skew the greyscale distribution. The higher the power law in either micro- or continuum-FE methods, the greater the effect of those artifacts.

As well as allowing the analysis of local trabecular behavior, the micro-FE method can produce useful results with average homogeneous material properties. In contrast the continuum-FE method requires the calibration of a conversion formula in order to create the material property map. This calibration requires the use of image phantoms and knowledge of the bone type, density, and specimen-preparation. The use of segmented BV/TV values rather than average greyscale is one way to eliminate some of the variability between cases.

15.4.4 Boundary Conditions

Sensitivity to boundary conditions is an issue for both micro- and continuum-FE models of bone. The choice of boundary conditions has been shown to have one the most significant effects on apparent stiffness values of all of the aspects studied in this chapter. It is easier to match model boundary conditions to experimental boundary conditions where the latter are more constrained. Matching frictional properties at free boundaries is challenging as these are often unknown. It is necessary to take care with the choice of boundary constraints: contact conditions, even when frictionless, can constrain movement more than simple nodal constraints.

15.4.5 Looking Forward

Both micro- and continuum-FE modeling techniques have advantages which should secure them a place in the virtual representation of trabecular bone for the foreseeable future. Continuum-FE can capture the inhomogeneity of the micro-structure sufficiently well to generate stiffness and strength predictions at a macro level, while keeping computational cost low enough to make whole bone models possible. In con-

trast the computational cost of micro-FE is high making it currently more suitable for the analysis of local behavior in small samples.

Information from sensitivity testing is a crucial aspect to be considered alongside experimental data on tissue properties and comparative validation studies, which together provide the necessary confidence in model predictions. The majority of the sensitivity tests reported for trabecular bone models consider overall stiffness as the output of interest. This trend is reflected in the studies detailed in this chapter. Establishing the accuracy of the overall stiffness prediction is a natural starting point for the development of these mechanical models of bone and is therefore the most well documented. However, advances in model sophistication are allowing the prediction of local behavior and the simulation of bone failure. These developments currently outstrip the availability of relevant sensitivity information. Sensitivity data, which quantifies the effect of key parameters on these alternative modeling outputs, will be an important part of next stage of evolution in this research area.

Conflict of Interest

The authors declare that they have no conflict of interest.

References

1. Anderson, A.E., Ellis, B.J., Weiss, J.A.: Verification, validation and sensitivity studies in computational biomechanics. *Comput. Methods Biomech. Biomed. Eng.* **10**(3), 171–184 (2007)
2. Austman, R.L., Milner, J.S., Holdsworth, D.W., Dunning, C.E.: The effect of the density-modulus relationship selected to apply material properties in a finite element model of long bone. *J. Biomech.* **41**, 3171–3176 (2008)
3. Bessho, M., Ohnishi, I., Matsuyama, J., Matsumoto, T., Imai, K., Nakamura, K.: Prediction of strength and strain of the proximal femur by a CT-based finite element method. *J. Biomech.* **40**, 1745–1753 (2007)
4. Bevill, G., Eswaran, S.K., Farahmand, F., Keaveny, T.M.: The influence of boundary conditions and loading mode on high-resolution finite element-computed trabecular tissue properties. *Bone* **44**, 573–578 (2009)
5. Bourne, B.C., van der Meulen, M.C.: Finite element models predict cancellous apparent modulus when tissue modulus is scaled from specimen CT-attenuation. *J. Biomech.* **37**, 613–621 (2004)
6. Boutroy, S., Van Rietbergen, B., Sornay-Rendu, E., Munoz, F., Bouxsein, M.L., Delmas, P.D.: Finite element analysis based on in vivo HR-pQCT images of the distal radius is associated with wrist fracture in postmenopausal women. *J. Bone Miner. Res.* **23**(3), 392–399 (2008)
7. Buckley, J.M., Loo, K., Motherway, J.: Comparison of quantitative computed tomography-based measures in predicting vertebral compressive strength. *Bone* **40**, 767–774 (2007)
8. Carlier, A., Van Oosterwyck, H., Geris, L.: *In Silico Biology of Bone Regeneration Inside Calcium Phosphate Scaffolds Tissue Engineering*, pp. 31–48. Springer, The Netherlands (2014)
9. Checa, S., Prendergast, P.J., Duda, G.N.: Inter-species investigation of the mechano-regulation of bone healing: comparison of secondary bone healing in sheep and rat. *J. Biomech.* **44**, 1237–1245 (2011)

10. Cifuentes, A., Kalbag, A.: A performance study of tetrahedral and hexahedral elements in 3-d finite element structural analysis. *Finite Elem. Anal. Des.* **12**, 313–318 (1992)
11. Cong, A., Buijs, J.O.D., Dragomir-Daescu, D.: In situ parameter identification of optimal density-elastic modulus relationships in subject-specific finite element models of the proximal femur. *Med. Eng. Phys.* **33**, 164–173 (2011)
12. d’Otreppe, V.: From medical imaging to finite element simulations: a contribution to mesh generation and locking-free formulations for tetrahedra. Ph.D. Thesis, University of Liege (2012)
13. d’Otreppe, V., Boman, R., Ponthot, J.-P.: Generating smooth surface meshes from multi-region medical images. *Int. J. Numer. Methods Biomed. Eng.* **28**, 642–660 (2012)
14. de Bien, C., Mengoni, M., d’Otreppe, V., Freichels, H., Jérôme, C., Ponthot, J.-P., Léonard, A., Toye, D.: Development of a biomechanical model of deer antler cancellous bone based on x-ray microtomographic images. In: *Proceedings of Micro-CT User Meeting*, pp. 137–145, 2012
15. Depalle, B., Chapurlat, R., Walter-Le-Berre, H., Bou-Saïd, B., Follet, H.: Finite element dependence of stress evaluation for human trabecular bone. *J. Mech. Behav. Biomed. Mater.* **18**, 200–212 (2013)
16. Ding, M., Odgaard, A., Hvid, I.: Accuracy of cancellous bone volume fraction measured by micro-CT scanning. *J. Biomech.* **32**, 323–326 (1999)
17. Eberle, S., Göttlinger, M., Augat, P.: An investigation to determine if a single validated density-elasticity relationship can be used for subject specific finite element analyses of human long bones. *Med. Eng. Phys.* **35**, 875–883 (2013)
18. Geris, L., Gomez-Cabrero, D.: An introduction to uncertainty in the development of computational models of biological processes. In: *Uncertainty in Biology, A Computational Modeling Approach*. Springer, Chem (2016, this volume)
19. Guldberg, R.E., Hollister, S.J., Charras, G.T.: The accuracy of digital image-based finite element models. *Trans. ASME J. Biomech. Eng.* **120**, 289–295 (1998)
20. Hara, T., Tanck, E., Homminga, J., Huiskes, R.: The influence of microcomputed tomography threshold variations on the assessment of structural and mechanical trabecular bone properties. *Bone* **31**, 107–109 (2002)
21. Harrison, N.M., McDonnell, P.F., O’Mahoney, D.C., Kennedy, O.D., O’Brien, F.J., McHugh, P.E.: Heterogeneous linear elastic trabecular bone modelling using micro-CT attenuation data and experimentally measured heterogeneous tissue properties. *J. Biomech.* **41**, 2589–2596 (2008)
22. Helgason, B., Perilli, E., Schileo, E., Taddei, F., Brynjólfsson, S., Viceconti, M.: Mathematical relationships between bone density and mechanical properties: a literature review. *Clin. Biomech.* **23**, 135–146 (2008)
23. Henninger, H.B., Reese, S.P., Anderson, A.E., Weiss, J.A.: Validation of computational models in biomechanics. *Proc. Inst. Mech. Eng. Part H J. Eng. Med.* **224**, 801–812 (2010)
24. Hojjat, S.-P., Beek, M., Akens, M.K., Whyne, C.M.: Can micro-imaging based analysis methods quantify structural integrity of rat vertebrae with and without metastatic involvement? *J. Biomech.* **45**, 2342–2348 (2012)
25. Homminga, J., Huiskes, R., Van Rietbergen, B., Rügsegger, P., Weinans, H.: Introduction and evaluation of a gray-value voxel conversion technique. *J. Biomech.* **34**, 513–517 (2001)
26. Jacobs, C.R., Davis, B.R., Rieger, C.J., Francis, J.J., Saad, M., Fyhrie, D.P.: The impact of boundary conditions and mesh size on the accuracy of cancellous bone tissue modulus determination using large-scale finite-element modeling. *J. Biomech.* **32**, 1159–1164 (1999)
27. Jones, A.C., Wilcox, R.K.: Assessment of factors influencing finite element vertebral model predictions. *Trans. ASME J. Biomech. Eng.* **129**, 898–903 (2007)
28. Keaveny, T.M., Pinilla, T.P., Crawford, R.P., Kopperdahl, D.L., Lou, A.: Systematic and random errors in compression testing of trabecular bone. *J. Orthopaed. Res.* **15**, 101–110 (1997)
29. Keaveny, T.M., Morgan, E.F., Niebur, G.L., Yeh, O.C.: Biomechanics of trabecular bone. *Annu. Rev. Biomed. Eng.* **3**, 307–333 (2001)

30. Kosmopoulos, V., Keller, T.S.: Predicting trabecular bone microdamage initiation and accumulation using a non-linear perfect damage model. *Med. Eng. Phys.* **30**, 725–732 (2008)
31. Ladd, A.J.C., Kinney, J.H.: Numerical errors and uncertainties in finite-element modeling of trabecular bone. *J. Biomech.* **31**, 941–945 (1998)
32. Matsuura, M., Eckstein, F., Lochmueller, E.-M., Zysset, P.K.: The role of fabric in the quasi-static compressive mechanical properties of human trabecular bone from various anatomical locations. *Biomech. Model. Mechanobiol.* **7**(1), 27–42 (2008)
33. Mengoni, M., Voide, R., de Bien, C., Freichels, H., Jérôme, C., Léonard, A., Toye, D., van Lenthe, G.H., Müller, R., Ponthot, J.-P.: A non-linear homogeneous model for bone-like materials under compressive load. *Int. J. Numer. Methods Biomed. Eng.* **28**(2), 334–348 (2012)
34. Morgan, E.F., Bayraktar, H.H., Keaveny, T.M.: Trabecular bone modulus-density relationships depend on anatomic site. *J. Biomech.* **36**, 897–904 (2003)
35. Müller, R., Rügsegger, P.: Three-dimensional finite element modelling of non-invasively assessed trabecular bone structures. *Med. Eng. Phys.* **17**, 126–133 (1995)
36. Niebur, G.L., Feldstein, M.J., Yuen, J.C., Chen, T.J., Keaveny, T.M.: High-resolution finite element models with tissue strength asymmetry accurately predict failure of trabecular bone. *J. Biomech.* **33**, 1575–1583 (2000)
37. Pahr, D.H., Zysset, P.K.: A comparison of enhanced continuum FE with micro FE models of human vertebral bodies. *J. Biomech.* **42**, 455–462 (2009)
38. Parkinson, I.H., Badiei, A., Fazzalari, N.L.: Variation in segmentation of bone from micro-ct imaging: implications for quantitative morphometric analysis. *Australas. Phys. Eng. Sci. Med.* **31**, 160–164 (2008)
39. Ramos, A., Simoes, J.: Tetrahedral versus hexahedral finite elements in numerical modelling of the proximal femur. *Med. Eng. Phys.* **28**, 916–924 (2006)
40. Rügsegger, P., Koller, B., Müller, R.: A microtomographic system for the nondestructive evaluation of bone architecture. *Calcif. Tissue Int.* **58**, 24–29 (1996)
41. Schulte, F.A., Zwahlen, A., Lambers, F.M., Kuhn, G., Ruffoni, D., Betts, D., Webster, D.J., Müller, R.: Strain-adaptive in silico modeling of bone adaptation: a computer simulation validated by in vivo micro-computed tomography data. *Bone* **52**, 485–492 (2013)
42. Schliemann-Bullinger, M., Fey, D., Bastogne, T., Findeisen, R., Scheurich, P., Bullinger, E.: The experimental side of parameter estimation. In: *Uncertainty in Biology, A Computational Modeling Approach*. Springer, Chem (2016, this volume)
43. Sikora, S.: *Experimental and Computational Study of the Behaviour of Trabecular Bone-Cement Interfaces*. PhD Thesis, University of Leeds, Leeds (2013)
44. Taddei, F., Cristofolini, L., Martelli, S., Gill, H.S., Viceconti, M.: Subject-specific finite element models of long bones: an in vitro evaluation of the overall accuracy. *J. Biomech.* **39**, 2457–2467 (2006)
45. Tarsuslugil, S.M., O’Hara, R.M., Dunne, N.J., Buchanan, F.J., Orr, J.F., Barton, D.C., Wilcox, R.K.: Development of calcium phosphate cement for the augmentation of traumatically fractured porcine specimens using vertebroplasty. *J. Biomech.* **46**, 711–715 (2013)
46. Taylor, R.L., Simo, J.C., Zienkiewicz, O.C., Chan, A.C.H.: The patch test: a condition for assessing FEM convergence. *Int. J. Numer. Methods Eng.* **22**, 39–62 (1986)
47. Ulrich, D., Van Rietbergen, B., Weinans, H., Rügsegger, P.: Finite element analysis of trabecular bone structure: a comparison of image-based meshing techniques. *J. Biomech.* **31**, 1187–1192 (1998)
48. Unnikrishnan, G.U., Morgan, E.F.: A new material mapping procedure for quantitative computed tomography-based continuum finite element analyses of the vertebra. *J. Biomech. Eng.* **133**(7), 071001 (2011)
49. Varga, P., Pahr, D.H., Baumbach, S., Zysset, P.K.: HR-pQCT based FE analysis of the most distal radius section provides an improved prediction of Colles’ fracture load in vitro. *Bone* **47**(5), 982–988 (2010)
50. Van Lenthe, G.H., Müller, R.: Prediction of failure load using micro-finite element analysis models: towards in vivo strength assessment. *Drug Discov. Today Technol.* **3**(2), 221–229 (2006)

51. Van Rietbergen, B., Weinans, H., Huiskes, R., Odgaard, A.: A new method to determine trabecular bone elastic properties and loading using micromechanical finite-element models. *J. Biomech.* **28**, 69–81 (1995)
52. Van Rietbergen, B., Weinans, H., Huiskes, R., Polman, B.J.W.: Computational strategies for iterative solutions of large fem applications employing voxel data. *Int. J. Numer. Methods Eng.* **39**, 2743–2767 (1996)
53. Wagner, D.W., Lindsey, D.P., Beaupre, G.S.: Deriving tissue density and elastic modulus from microCT bone scans. *Bone* **49**, 931–938 (2011)
54. Wijayathunga, V.N., Jones, A.C., Oakland, R.J., Furtado, N.R., Hall, R.M., Wilcox, R.K.: Development of specimen-specific finite element models of human vertebrae for the analysis of vertebroplasty. *Proc. Inst. Mech. Eng. Part H-J. Eng. Med.* **222**, 221–228 (2008)
55. Wolfram, U., Wilke, H.J., Zysset, P.K.: Valid μ finite element models of vertebral trabecular bone can be obtained using tissue properties measured with nanoindentation under wet conditions. *J. Biomech.* **43**, 1731–1737 (2010)
56. Zhao, Y.: Finite Element Modelling of Cement Augmentation and Fixation for Orthopaedic Applications. Ph.D. Thesis, University Of Leeds, Leeds (2010)
57. Zöllner, A.M., Tepole, A.B., Kuhl, E.: On the biomechanics and mechanobiology of growing skin. *J. Theor. Biol.* **297**, 166–175 (2012)
58. Zysset, P.K.: A review of morphology-elasticity relationships in human trabecular bone: theories and experiments. *J. Biomech.* **36**(10), 1469–1485 (2003)